Neuroprotection by cyclodextrin in cell and mouse models of Alzheimer disease

Jiaqi Yao,[1] Daniel Ho,[1] Noel Y. Calingasan,[1] Nina H. Pipalia,[2] Michael T. Lin,[1] and M. Flint Beal[1]

[1]Department of Neurology and Neuroscience and [2]Department of Biochemistry, Weill Cornell Medical College, New York, NY 10065

There is extensive evidence that cholesterol and membrane lipids play a key role in Alzheimer disease (AD) pathogenesis. Cyclodextrins (CD) are cyclic oligosaccharide compounds widely used to bind cholesterol. Because CD exerts significant beneficial effects in Niemann-Pick type C disease, which shares neuropathological features with AD, we examined the effects of hydroxypropyl-β-CD (HP-β-CD) in cell and mouse models of AD. Cell membrane cholesterol accumulation was detected in N2a cells overexpressing Swedish mutant APP (SwN2a), and the level of membrane cholesterol was reduced by HP-β-CD treatment. HP-β-CD dramatically lowered the levels of Aβ42 in SwN2a cells, and the effects were persistent for 24 h after withdrawal. 4 mo of subcutaneous HP-β-CD administration significantly improved spatial learning and memory deficits in Tg19959 mice, diminished Aβ plaque deposition, and reduced tau immunoreactive dystrophic neurites. HP-β-CD lowered levels of Aβ42 in part by reducing β cleavage of the APP protein, and it also up-regulated the expression of genes involved in cholesterol transport and Aβ clearance. This is the first study to show neuroprotective effects of HP-β-CD in a transgenic mouse model of AD, both by reducing Aβ production and enhancing clearance mechanisms, which suggests a novel therapeutic strategy for AD.

CORRESPONDENCE
Jiaqi Yao:
jiy2006@med.cornell.edu
OR
M. Flint Beal:
fbeal@med.cornell.edu

Abbreviations used: AD, Alzheimer's disease; CatD, cathepsin D; CD, cyclodextrins; HP-β-CD, hydroxypropyl-β-CD; CTF, C-terminal fragment; LXR, liver X receptor; NOC1, Niemann-Pick type C1; SREBP, terol regulatory element binding proteins; SwN2a, N2a cells overexpressing Swedish mutant APP; ThS, Thioflavin S.

There is extensive evidence implicating cholesterol in the pathogenesis of AD. Epidemiological studies have shown that hypercholesterolemia is an important risk factor for AD (Kivipelto et al., 2001; Puglielli et al., 2003). Furthermore, higher cholesterol levels are observed in the brains of AD patients (Xiong et al., 2008). Cholesterol is a major component of the lipid bilayer membrane, where β- and γ-secretases are located. β-C-terminal fragments (β-CTFs), which are the products of β cleavage of the amyloid precursor protein (APP), directly bind cholesterol (Barrett et al., 2012). Increased cellular cholesterol increases the association of APP with β- and γ-secretases in cholesterol-rich lipid rafts, which stimulates cleavage of APP into Aβ (Lee et al., 1998; Ehehalt et al., 2003; Xiong et al., 2008; Kodam et al., 2010; Vetrivel and Thinakaran, 2010).

Cholesterol homeostasis is tightly regulated by feedback mechanisms: sterol regulatory element binding proteins (SREBPs) and liver X receptors (LXRs) regulate the expression of genes that control the uptake, synthesis, and export of cholesterol. SREBPs regulate the expression of genes encoding HMG-CoA reductase and HMG-CoA synthase, which play essential roles in cholesterol synthesis (Brown and Goldstein, 1997; Bełtowski, 2008; Sato, 2010). LXRs activate genes encoding the ATP-binding cassette subfamily A/G transporters (ABCA/Gs), which control cholesterol efflux across the plasma membrane to apolipoprotein acceptors, initiating the reverse cholesterol transport pathway (Schmitz and Drobnik, 2002; Jessup et al., 2006). Studies in mouse models of AD indicate that ABCA1 plays an important role in the induction of ApoE lipidation, in facilitating Aβ transport to ApoE-containing carriers for clearance, and in suppression of Aβ generation. Disruption of ABCA1 leads to increased insoluble Aβ and parenchymal amyloid plaques, with no change in APP processing (Hirsch-Reinshagen et al., 2005; Koldamova et al., 2005a; Wahrle et al., 2005; Kim et al., 2007; Cramer et al., 2012).

The Rockefeller University Press $30.00
J. Exp. Med. 2012 Vol. 209 No. 13 2501-2513
www.jem.org/cgi/doi/10.1084/jem.20121239

The Journal of Experimental Medicine

Activation of LXRs produces behavioral improvement and removal of fibrillar Aβ in transgenic mouse models expressing mutant APP (Koldamova et al., 2005b; Terwel et al., 2011).

Cyclodextrins (CDs) are a family of cyclic polysaccharide compounds that can extract cholesterol from cultured cells (Zidovetzki and Levitan, 2007; Coskun and Simons, 2010; Di Paolo and Kim, 2011). In transgenic mouse models of the

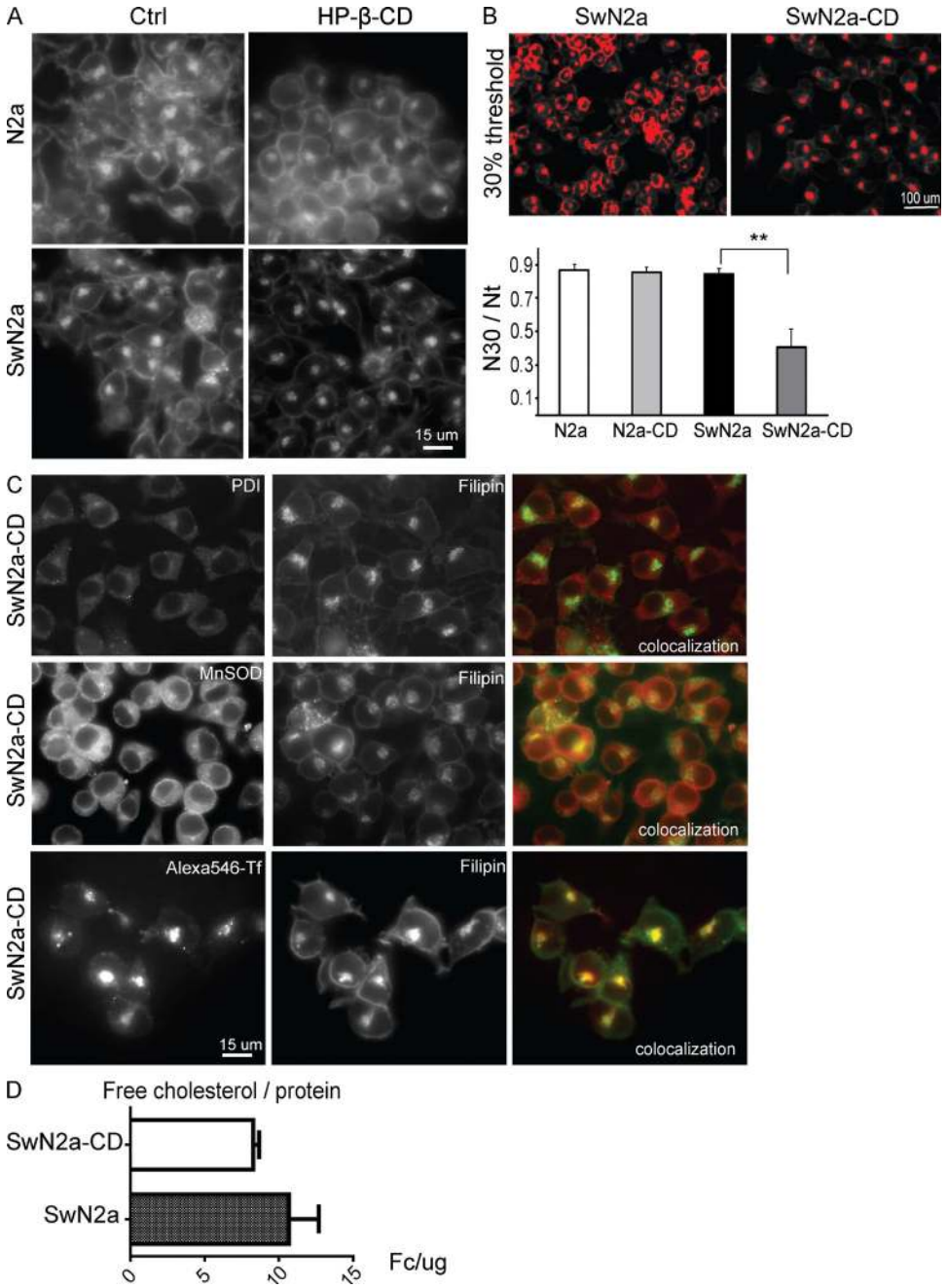

Figure 1. HP-β-CD reduces membrane cholesterol and alters cholesterol distribution in SwN2a cells. (A) Filipin staining of N2a cells and SwN2a cells treated with and without 5 mM HP-β-CD. Bar, 15 µm. (B) A 70% threshold (leaving the top 30% of intensities in red) was applied to the images to visualize the level of high-intensity filipin staining. The number of cells with the top 30% of cholesterol intensity (N30) and the number of total cells (Nt) were counted. Cells were analyzed from different dishes (n = 5 each). The ratio between N30/Nt is shown. **, $P < 0.01$. (C) Double staining of filipin and markers for intracellular compartments (endoplasmic reticulum, PDI; mitochondria, MnSOD; endosomal recycling compartment, transferrin) in SwN2a cells treated with 5 mM HP-β-CD. (D) Cholesterol (Free cholesterol Fc) was extracted from SwN2a cells treated with and without HP-β-CD, measured by GC mass spectrometry, and normalized to total protein amount (micrograms). $P = 0.05$. Each experiment was performed at least three times independently.

lipid storage disease Niemann-Pick type C1 (NPC1), subcutaneous administration of CDs improved cholesterol trafficking, corrected abnormal cholesterol metabolism, and prevented neurodegenerative changes in NPC1$^{-/-}$ mice (Liu et al., 2008, 2010; Zhang et al., 2009; Ramirez et al., 2010; Aqul et al., 2011). Notably, intriguing parallels exist between NPC1 and AD, including neurofibrillary tangles and prominent lysosomal system dysfunction (Nixon, 2004; Liu et al., 2010). A recent study showed that CDs reversed attenuated behavioral and pathological abnormalities in a mouse model generated by crossing NPC1$^{+/-}$ mice with mutant APP transgenic mice (Maulik et al., 2012). It is therefore plausible that CDs may also benefit AD (Aqul et al., 2011). In vitro studies showed that CDs reduce membrane cholesterol levels and reduce both BACE and γ-secretase activities (Hartmann et al., 2007), leading to additive effects in reducing amyloid-β production (Simons et al., 1998).

In this study, we examined the hydroxypropyl form of β-CD (HP-β-CD) in Tg19959 mice, which overexpress human APP with the Swedish and Indiana familial AD mutations. These mice robustly develop Aβ pathology and memory deficits at 3–4 mo of age (Yao et al., 2010). We injected the mice subcutaneously with HP-β-CD starting at 7 d of age, twice weekly until 4 mo of age. Treatment with HP-β-CD significantly reduced Aβ burden and phosphorylated tau pathology, and improved memory in the Morris water maze. HP-β-CD activated expression of genes, including ABCA1, suggesting that HP-β-CD increases cholesterol transport and enhances Aβ clearance.

RESULTS

HP-β-CD reduced cell membrane cholesterol and amyloid-β production in a cell model overexpressing APP

Using the cholesterol probe filipin, we detected cholesterol at cell membranes (Fig. 1 A) in N2a cells and N2a cells overexpressing mutant human APP (SwN2a). There was no significant difference in cholesterol staining between N2a and SwN2a cells at baseline (Fig. 1 A). After treating cells with 5 mM HP-β-CD for 30 min (Simons et al., 1998), a significant reduction of membrane cholesterol was observed in SwN2a cells, and there were more intracellular compartments positive for filipin in SwN2a cells as compared with N2a cells (Fig. 1 A). To quantify high-intensity filipin staining, a threshold was applied to the images (Guirland et al., 2004; Yao et al., 2006). High-intensity staining for cholesterol occurred at cell membranes, and the fraction of cells with high-intensity membrane cholesterol staining was significantly reduced after HP-β-CD treatment in SwN2a cells, but not in N2a cells (Fig. 1 B). To identify the filipin-positive intracellular compartments seen in SwN2a cells after HP-β-CD treatment, we double stained with filipin and several intracellular markers. The best colocalization was observed between filipin and transferrin (Tf), a classical marker of endocytic recycling compartments (ERCs; Fig. 1 C). We also measured total cholesterol by gas chromatography-mass spectrometry, and HP-β-CD treatment decreased total cholesterol in SwN2a cells ($P = 0.05$; Fig. 1 D).

The key proteins involved in Aβ production are membrane proteins. HP-β-CD reduces the level of membrane cholesterol, and this in turn has effects on the composition and motility of membranes. To test if HP-β-CD changed Aβ production, SwN2a cells were treated with 5 mM HP-β-CD for 30 and 60 min, followed by 5 and 24 h, respectively, of incubation in serum-free medium to recover. The cell medium and cell extracts were tested for levels of Aβ42, measured by ELISA (Fig. 2). HP-β-CD treatment significantly reduced the levels of both extracellular and intracellular Aβ42 in SwN2a cells, and the effects persisted for 24 h. Extracts from SwN2a cells were also analyzed by Western blot. HP-β-CD decreased levels of APP β-C-terminal fragments (CTFs; unpublished data), which suggests reduced β-cleavage of APP.

HP-β-CD improved learning and memory in Tg19959 mice

Although HP-β-CD penetrates the blood–brain barrier at a low rate in mature mice (Aqul et al., 2011; Ramirez et al., 2011;

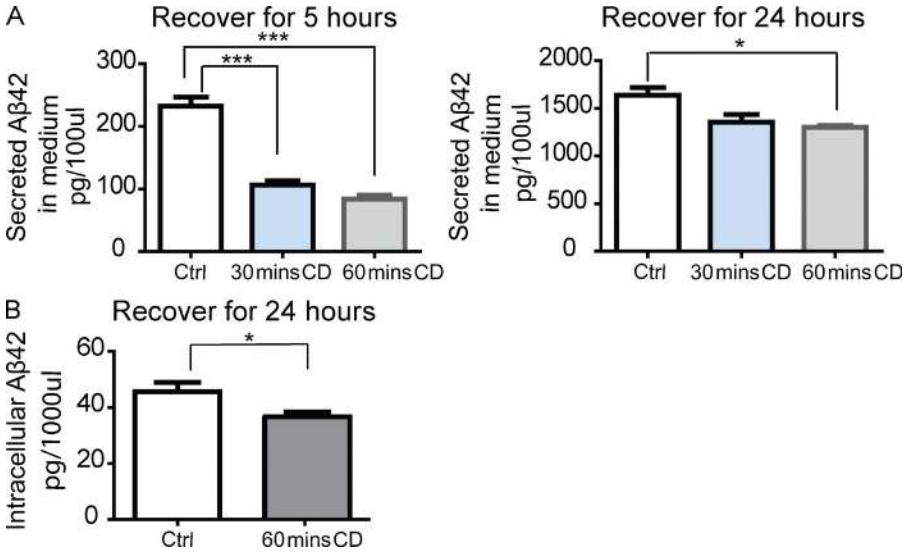

Figure 2. HP-β-CD treatment significantly reduces levels of Aβ42 in vitro. (A) SwN2a cells were treated with 5 mM HP-β-CD for 30 and 60 min, followed by incubation in serum-free media for 5 or 24 h. Media were collected, and levels of Aβ42 were measured by ELISA. (B) The levels of intracellular Aβ42 in SwN2a cells treated with 5 mM HP-β-CD for 60 min were measured by ELISA. *, $P < 0.05$; ***, $P < 0.001$; $n = 4$ wells of cells for each condition. Experiments were performed at least two times independently.

Peake and Vance, 2012), administration of HP-β-CD prevents neurodegeneration in a mouse model of NPC1 (Liu et al., 2008, 2010; Davidson et al., 2009; Aqul et al., 2011). We therefore used the same method and dosage to treat Tg19959 (Tg) mice and WT littermate mice starting at postnatal day 7 (P7). The HP-β-CD solution or saline control was administrated to the mice subcutaneously twice a week using a dose of 4,000 mg/kg. To test if HP-β-CD improved cognitive deficits, 4-mo-old Tg and WT mice treated with or without HP-β-CD were examined using the Morris water maze (MWM), a hippocampus-dependent memory test. WT mice learned and associated spatial cues with the location of the hidden platform, and reached the platform in 15 s in the training session (Fig. 3 A, open circles). Tg mice exhibited severe learning deficits in the training phase (Fig. 3 A, open squares) as compared with WT littermates ($P < 0.001$). HP-β-CD treatment improved learning in the Tg mice (Fig. 3 A, filled squares; $P = 0.05$), but it had no significant effect in WT mice (Fig. 3 A, filled circles). In the probe trial, HP-β-CD–treated Tg mice showed markedly better memory, indicated by spending a longer time in the platform region, compared with Tg mice treated with saline ($P < 0.01$; Fig. 3 B, left graph). There were no differences among the groups in swimming speed (Fig. 3 B, right graph) or locating the visible platform (Fig. 3 C), excluding motor and visual issues as causes of the improvement by HP-β-CD treatment.

HP-β-CD significantly reduced Aβ plaque load and microgliosis in Tg19959 mice

To determine the effects of HP-β-CD on Aβ deposition, brain sections from 4-mo-old Tg19959 mice treated with and without HP-β-CD were immunostained with an anti-Aβ42 antibody. Aβ42-immunoreactive plaques were robustly detected in brains of Tg19959 mice (Fig. 4 A). HP-β-CD treatment significantly reduced the percentage of brain area occupied by Aβ plaques in both cerebral cortex ($P < 0.001$) and hippocampus ($P < 0.01$) of Tg19959 mice (Fig. 4, A and B). To further characterize the nature of the deposited Aβ plaques, brain sections were stained with Thioflavin S (ThS), which selectively detects fibrillar, but not diffuse, Aβ deposits. Like the anti-Aβ antibody staining, HP-β-CD–treated Tg19959 mice had significantly fewer ThS-positive fibrillar plaques as compared with the control group ($P < 0.0001$; Fig. 4, C and D). Thus, HP-β-CD administration decreases total and fibrillar Aβ deposition in Tg19959 mice.

Another major characteristic of AD pathology is an increased inflammatory response as indicated by increased

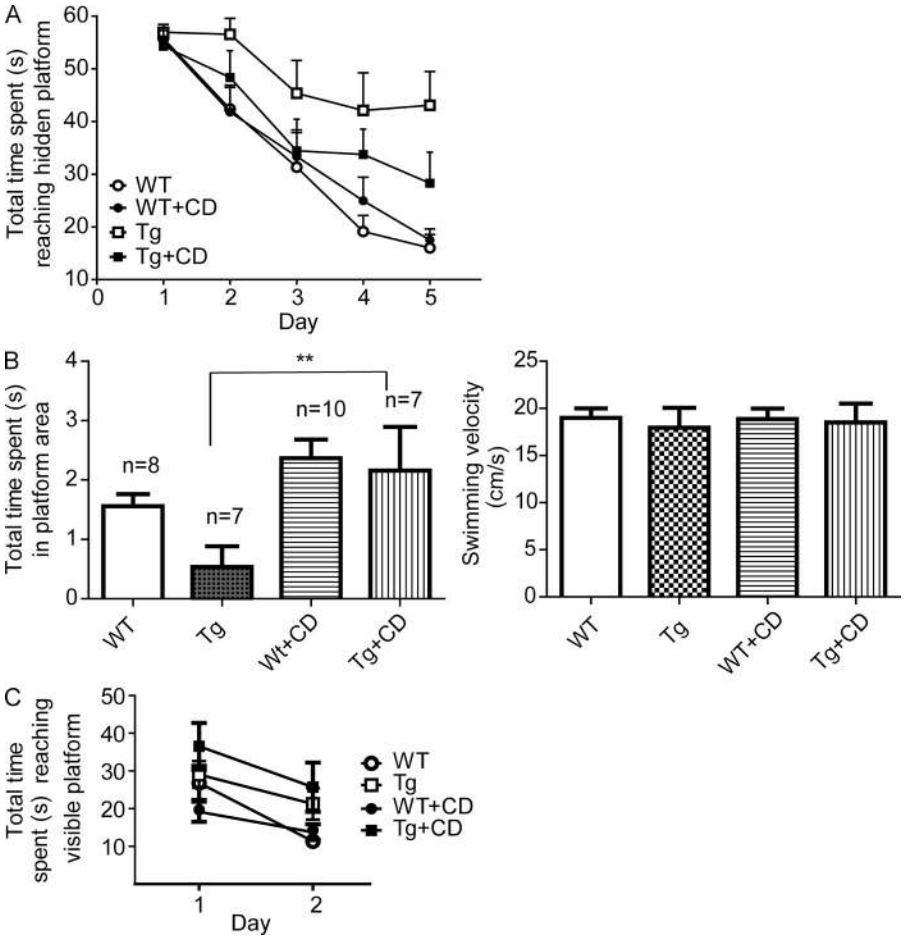

Figure 3. HP-β-CD treatment significantly improves spatial learning and memory in Tg19959 mice tested in Morris water maze. (A) Time before reaching the hidden platform during five days of training. (B, left) Total time spent in the platform area during probe trial. **, $P < 0.01$. (right) Swimming velocity during the probe trial. (C) Total time before reaching the visible platform during two days with visible platform. n = 7–10 in each group. Morris water maze results were obtained from one cohort.

microgliosis (Wyss-Coray, 2006). Previous studies suggested that amyloid plaques may trigger neuroinflammatory cascades (Meyer-Luehmann et al., 2008). To quantitatively examine the extent of microgliosis, we used immunostaining with the CD11b antibody. We found a dramatic reduction of microgliosis in cerebral cortex ($P < 0.01$) and hippocampus ($P = 0.05$) of Tg19959 mice treated with HP-β-CD as compared with the control group (Fig. 4, E and F). These findings demonstrate that HP-β-CD administration reduces Aβ plaque deposition and decreases microgliosis.

HP-β-CD decreased Aβ production and amyloidogenic processing of APP in Tg19959 mice

HP-β-CD decreased Aβ levels and β-secretase cleavage of APP in SwN2a cells. To investigate Aβ levels and APP processing in vivo, protein was extracted from brains of Tg19959 mice treated with and without HP-β-CD and subjected to Western blotting. To detect Aβ, the 6E10 antibody was used (Fig. 5 A). Tubulin was used as a loading control. Levels of Aβ were significantly reduced in the brains of Tg19959 mice treated with HP-β-CD ($P < 0.05$). The same extract was also analyzed quantitatively for Aβ42 and Aβ40 by ELISA. Levels of both Aβ42 and Aβ40 per brain weight were significantly reduced in Tg19959 mice treated with HP-β-CD (Fig. 5 B; $P < 0.05$). We also examined the levels of APP CTFs, using the 6E10 and APP C-terminal antibodies (Fig. 5, C and D). Both antibodies recognize β-CTFs, but only the APP C-terminal antibody recognizes α-CTFs. As shown in Fig. 5 C, HP-β-CD treatment did not affect full-length APP (short exposure time with 6E10), but it significantly lowered the level of β-CTFs ($P < 0.05$). The levels of α-CTFs, normalized to tubulin, were not changed significantly by HP-β-CD (Fig. 5 D). Thus, HP-β-CD decreased brain Aβ levels in vivo, at least in part by reducing amyloidogenic processing of APP.

HP-β-CD reduced tau pathology in the brains of Tg19959 mice

Dystrophic neurites are abnormal neuronal processes that are associated with Aβ plaques (Dickson et al., 1999) and play a critical role in AD pathogenesis. In the brains of Tg19959 mice, dystrophic neurites are immunopositive with an antibody (AT8) that detects tau phosphorylated at both serine 202 and threonine 205. Both cerebral cortex and hippocampus showed AT8-positive dystrophic neurites in Tg19959

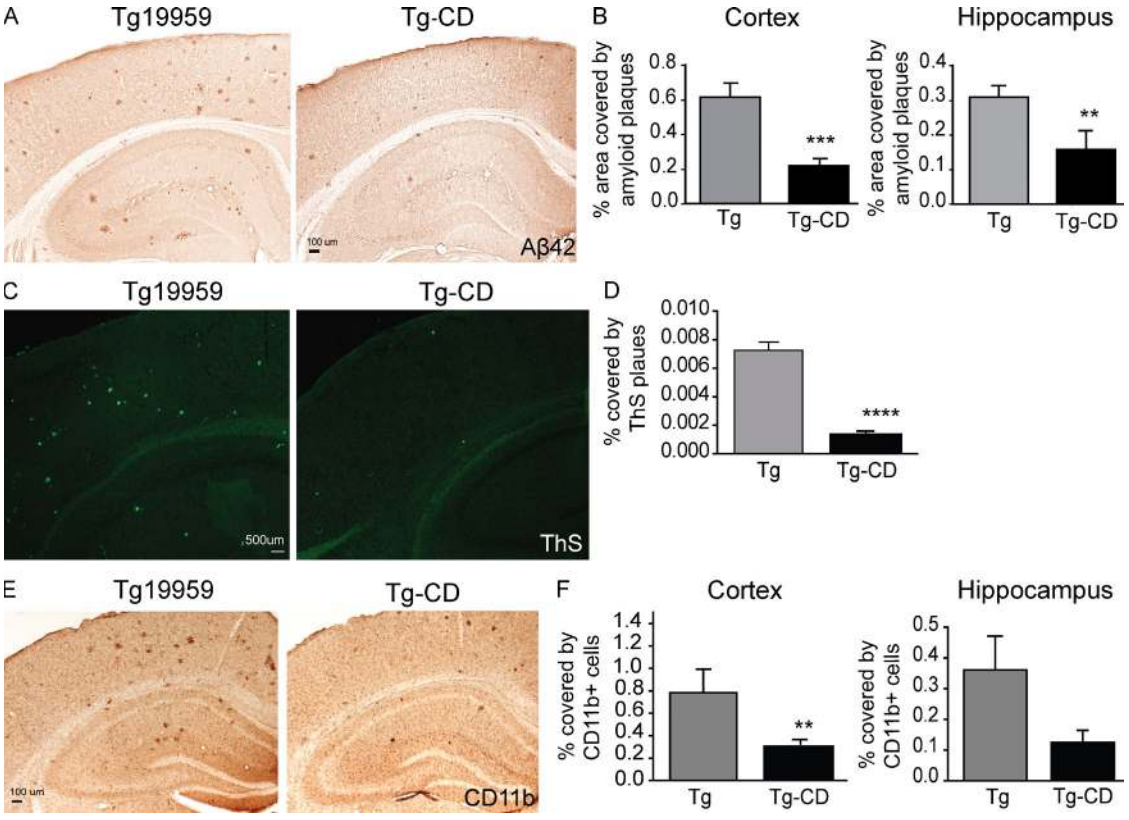

Figure 4. HP-β-CD treatment significantly reduces amyloid plaque burden and microgliosis in Tg19959 mice at 4 mo of age. (A) Representative images of amyloid plaques detected with an Aβ42 antibody. (B) Percentage of area covered by amyloid plaques in cerebral cortex and hippocampus in Tg19959 mice treated with saline or HP-β-CD. (C) Representative images of amyloid plaques stained with ThS. (D) Percentage of area covered by ThS-positive plaques. (E) Representative images of reactive microglia detected with a CD11b antibody. (F) Percentage of area covered by reactive microglia in Tg19959 mice treated with saline or HP-β-CD. *, $P < 0.05$; ***, $P < 0.001$; ****, $P < 0.0001$; $n = 9–10$ in each group. All results were obtained and analyzed from two separate animal studies.

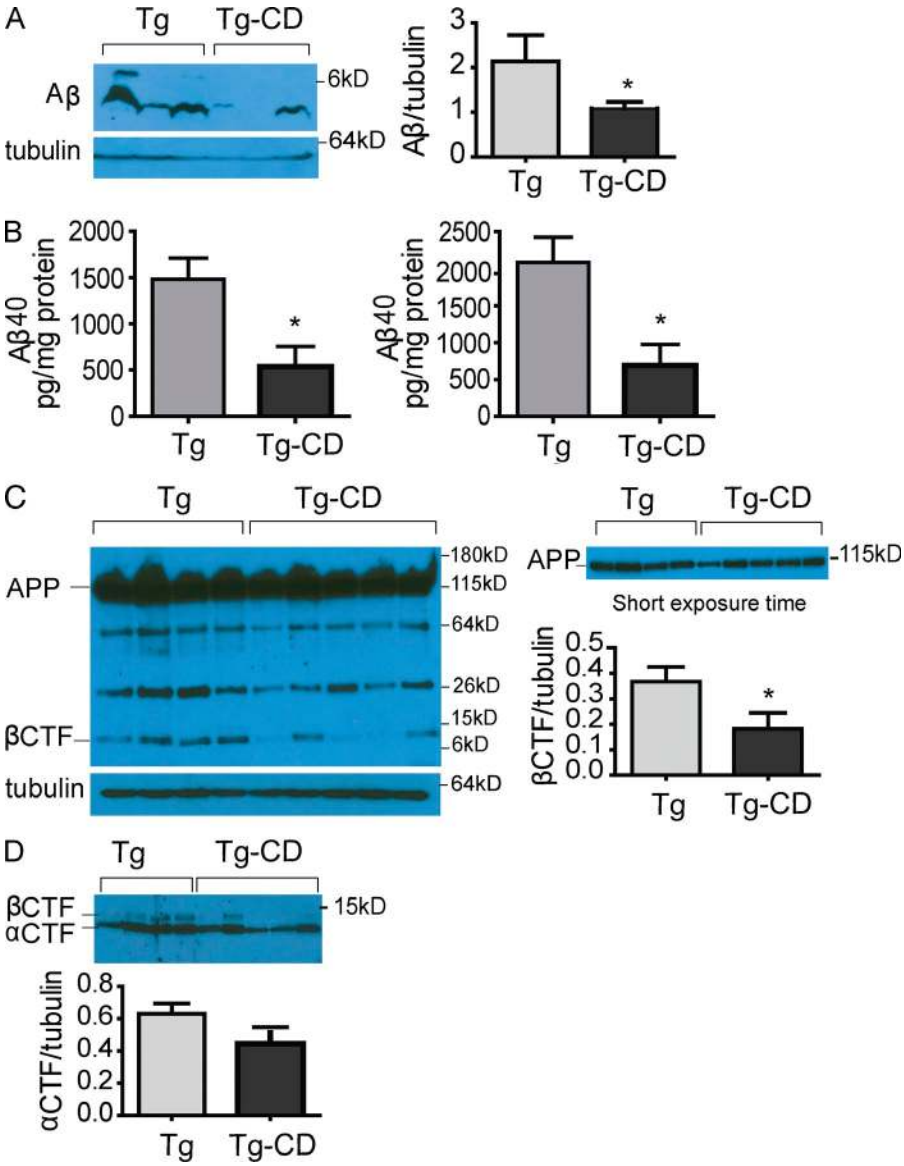

Figure 5. HP-β-CD treatment prominently reduces the levels of Aβ in brain extracts from Tg19959 mice. (A) Representative image of Western blots of Aβ, detected with 6E10 antibody and normalized to tubulin. *, $P < 0.05$. (B) Levels of Aβ42 and Aβ40 examined by ELISA. *, $P < 0.05$. (C) Western blots of β-CTFs (left gel) using 6E10 antibody. Short exposure image shows full-length APP. The levels of β-CTFs were normalized to tubulin. (D) The same membrane stripped and re-blotted with an APP C-terminal antibody to show α- and β-CTFs. $n = 4$ (Tg); $n = 7$ (Tg-CD). All results were analyzed from two separate animal studies.

mice, particularly around plaques (Fig. 6, A and C). Interestingly, HP-β-CD–treated Tg19959 mice showed a significant reduction in the area occupied by AT8-positive immunostaining by about twofold in the cerebral cortex and by over sixfold in the hippocampus. Because neuronal processes and synapses play an important role in cognition, the improvement of cognitive function after HP-β-CD treatment in Tg19959 mice may be a consequence of reducing the numbers of dystrophic neurites.

HP-β-CD corrected lysosomal abnormalities in the brains of Tg19959 mice

Lysosomal abnormalities have been shown to be closely related to AD pathogenesis (Bahr et al., 1994; Nixon et al., 2000; Zhang et al., 2009; Yang et al., 2011). Enlarged lysosomes immunopositive for the lysosomal marker cathepsin D (CatD) are seen in the brains of APP transgenic mice similar to Tg19959 mice (Yang et al., 2011). We therefore examined cathepsin D immunostaining in the brains of WT and Tg mice using the antibody RU4 (gift from R. Nixon, New York University School of Medicine/Nathan Kline Institute, New York, NY). Consistent with the previous work, we observed abnormal cathepsin D–positive accumulation in the brains of 4-mo-old Tg19959 mice (Fig. 6 E, top left) compared with WT mice (not depicted). HP-β-CD administration decreased the abnormal cathepsin D staining in the brains of Tg19959 mice (Fig. 6 E, top right). A threshold was applied to all the images, to allow quantification of high intensity cathepsin D immunostaining (Fig. 6 E, top; Guirland et al., 2004; Yao et al., 2006). HP-β-CD administration significantly reduced high-intensity cathepsin D immunostaining in the brains of Tg19959 mice (Fig. 6 F). Because the abnormal accumulation of lysosomes may be a compensatory response to the elevated levels of Aβ in AD, the reduction of

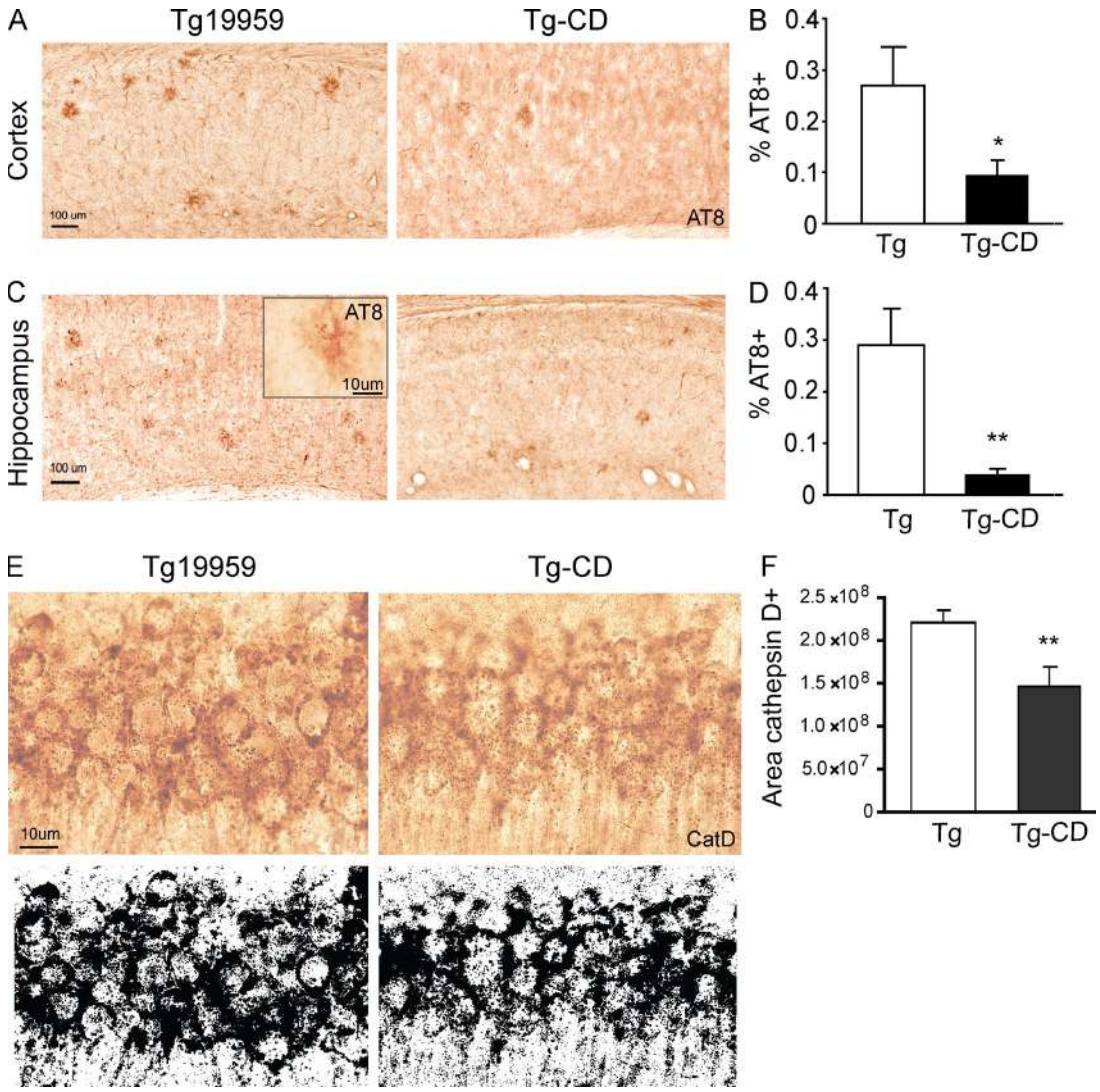

Figure 6. Pathological markers of AD were reduced in Tg19959 mice treated with HP-β-CD compared with saline. (A and C) Representative images of AT8 immunostaining in the cerebral cortex and hippocampus. Bar, 100 µm. Inset shows higher magnification of AT8 staining in dystrophic neurites. Bar, 10 µm. (B and D) Percentage of area covered by AT8 immunostaining in HP-β-CD–treated Tg19959 mice. n = 9–10 in each group. *, $P < 0.05$; **, $P < 0.001$. All results were obtained and analyzed from two separate animal studies. (E) Brain sections from 4-mo-old Tg19959 and Tg19959 mice treated with HP-β-CD immunostained with an antibody against cathepsin D (RU4, top). A threshold was applied to the images (bottom). Bar, 10 µm. (F) Graph of the area covered with high-intensity cathepsin D immunostaining. n = 4–5 mice; 5 slices/mouse were examined. **, $P < 0.001$.

Aβ levels produced by HP-β-CD treatment may result in a decrease of the abnormal lysosomal accumulation (Zhang et al., 2009).

HP-β-CD treatment up-regulates genes involved in cholesterol trafficking

Cholesterol regulates gene expression at the transcriptional level, and two key transcription factors that have been implicated are the sterol regulatory element binding protein (SREBP) and the liver X receptor (LXR; Maxwell et al., 2003). SREBP-2 preferentially activates genes involved in cholesterol synthesis and metabolism, such as HMG-CoA synthase and HMG-CoA reductase. LXRs control genes involved in sterol movement across membranes, including ABCAs, ABCGs, and NPCs (Fontaine et al., 2008).

We examined the mRNA levels of genes that are involved in cholesterol transport and metabolism (Fig. 7). Brain tissue was collected after the mice were tested in the MWM, 8 d after the last HP-β-CD injection. In the brains of Tg19959 mice, chronic HP-β-CD administration significantly increased mRNA levels of *abca1* and *npc1* (Fig. 7, A and D; $P < 0.05$). We also observed a trend toward increased mRNA levels of *npc1* in Tg19959 mice compared with WT mice. This is consistent with a recent study showing increased *npc1* expression in APP/PS1 mice and in AD patients (Kågedal et al., 2010). There were no significant

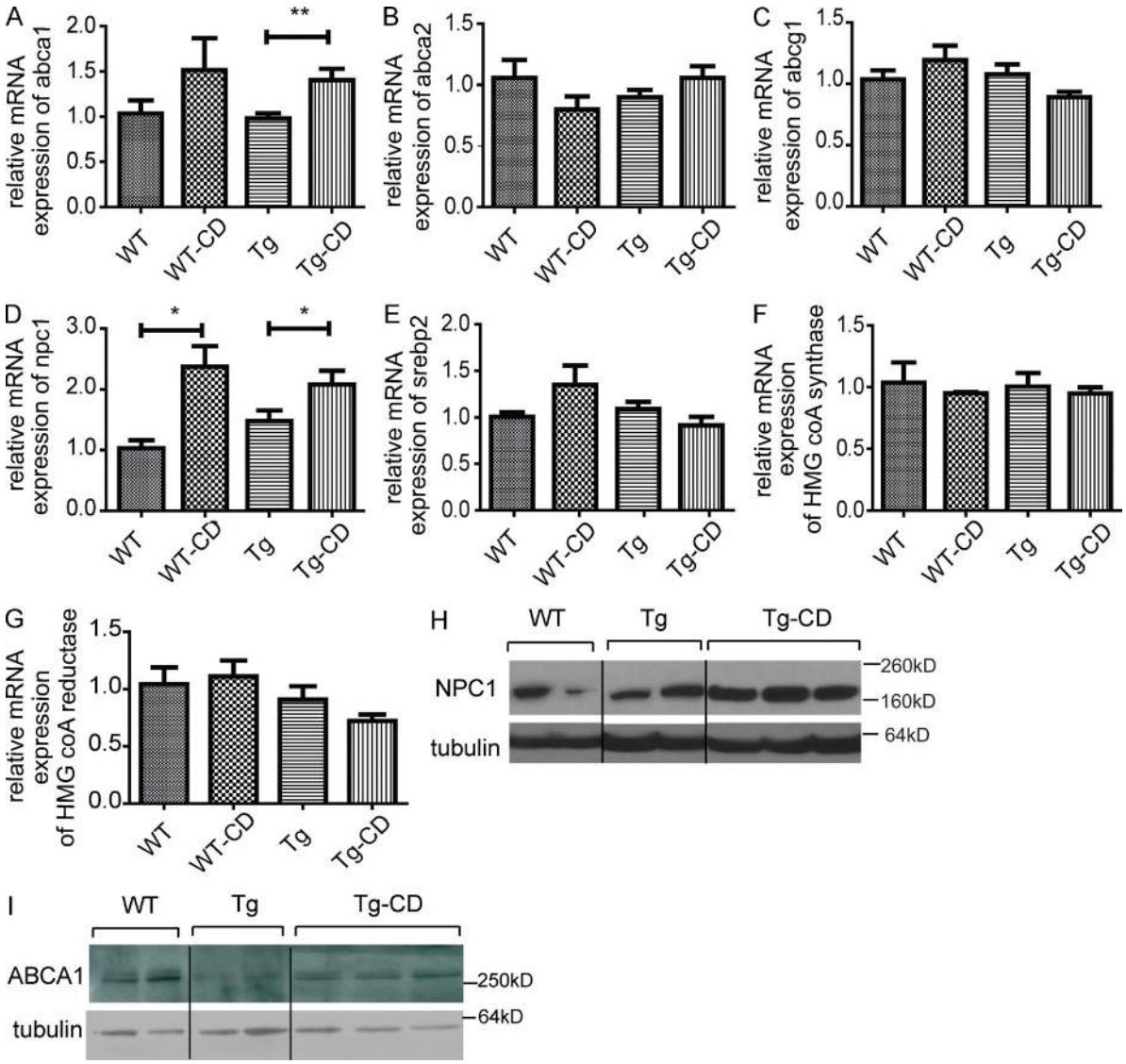

Figure 7. Expression levels of genes involved in lipid trafficking and metabolism in the brains of Tg19959 mice and WT littermates treated with and without HP-β-CD. (A–G) Relative expression levels of mRNAs normalized to the levels of actin. $n = 7–10$ in each group. *, $P < 0.05$; **, $P < 0.01$. All results were obtained and analyzed from two separate animal studies. (H and I) Representative Western blots of NPC1 and ABCA1 compared with tubulin in the brains of Tg19959 mice treated with and without HP-β-CD.

changes in mRNA levels of *abca2* or *abcg1* (Fig. 7, B and C). There were also no changes in mRNA levels of *srebp*2, *hmg-CoA synthase*, or *hmg-CoA reductase* among the groups (Fig. 7, E–G). Thus, long-term HP-β-CD treatment increased levels of genes that play critical roles in transporting lipids, and in turn may elevate cholesterol trafficking out of cells. Protein levels of ABCA1 and NPC1 were also elevated in the brains of Tg19959 treated with HP-β-CD (Fig. 7, H and I). Notably, ABCA1 is involved not only in cholesterol efflux, but also in increasing ApoE lipidation and improving Aβ clearance (Hirsch-Reinshagen et al., 2005; Koldamova et al., 2005a; Wahrle et al., 2005, 2008; Cramer et al., 2012). Our data suggest that long-term HP-β-CD administration to Tg19959 mice increases expression of genes that are involved in cholesterol efflux, and may enhance ABCA1-mediated Aβ clearance by astrocytes.

DISCUSSION

Disturbed cholesterol homeostasis plays an important role in AD pathogenesis. Although interventional studies using statins were unsuccessful (Jick et al., 2000; Blauw et al., 2001; McGuinness et al., 2009; Sparks et al., 2010), epidemiological studies show that high cholesterol levels are associated with an increased incidence of AD (Kivipelto et al., 2001). Furthermore, there is extensive laboratory evidence which shows that neuronal cholesterol promotes Aβ production, and that

modulation of cholesterol levels exerts beneficial effects in both in vitro and in vivo models of AD (Simons et al., 1998; Wahrle et al., 2002; Cordy et al., 2006; Barrett et al., 2012). We observed increased cholesterol staining around plaques in Tg19959 mice (unpublished data).

Aβ generation involves cleavage of the transmembrane protein APP by β-secretase in the luminal domain, followed by cleavage by γ-secretase within the transmembrane domain. APP and the β- and γ-secretases are colocalized in cholesterol rich "lipid rafts," so membrane cholesterol plays a key role in APP processing. We observed that HP-β-CD treatment reduces total cholesterol, likely by direct extraction, and redistributes cholesterol from the plasma membrane to intracellular compartments, particularly ERCs. Studies of sterol trafficking have demonstrated that cholesterol can be transferred from cell membrane to ERCs within seconds, with ERCs acting as a "sink" to store cholesterol (Mesmin and Maxfield, 2009; Mondal et al., 2009). These effects likely reduce cholesterol-rich lipid rafts available for APP processing. It was recently shown that cholesterol directly binds to APP and promotes Aβ production (Barrett et al., 2012), so it is therefore plausible that lowering membrane cholesterol could directly affect APP processing and reduce Aβ production. Our results confirmed that HP-β-CD significantly decreased both β-CTF levels and intracellular and extracellular Aβ42 levels in SwN2a cells, and the effect persisted 24 h after initial HP-β-CD treatment. Importantly, administration of HP-β-CD to Tg19959 mice also significantly lowered β-CTF levels and Aβ production in vivo. We should note that the beneficial effects on Aβ and behavior observed in vivo may not occur by the same mechanisms as the beneficial effects seen in vitro. Brain in vivo is exposed to only a small fraction of the HP-β-CD administered systemically, whereas cells in vitro are exposed directly to higher concentrations of HP-β-CD. One possibility is that the lower concentrations of HP-β-CD in brain are sufficient to produce the effects observed. Alternatively, HP-β-CD might act primarily to reduce Aβ outside the brain, thereby reducing brain Aβ by a "peripheral sink" mechanism similar to that postulated for Aβ-directed immunotherapy (Morgan, 2011). Still, we observed reduced β-CTF levels in brain, suggesting that HP-β-CD exerts beneficial effects at least in part by reducing amyloidogenic processing of APP in brain.

An interesting finding in this study is that HP-β-CD treatment elevates the expression levels of genes encoding ABCA1 and NPC1. NPC1 is located in endosomal/lysosomal compartments, and is responsible for cholesterol trafficking between the endosomal/lysosomal compartments and cytoplasm. ABCA1, a membrane cholesterol transporter, mediates reverse cholesterol transport, which transfers cholesterol onto apolipoproteins and forms pre-HDL particles for excretion. Collectively, our results suggest that administration of HP-β-CD may enhance cholesterol efflux through increased expression of cholesterol transporters.

Another important function of ABCA1 is its key role in apoE lipidation and, subsequently, in the process of Aβ clearance. Mice lacking ABCA1 (*abca1*$^{-/-}$) have abnormally small apoE-containing lipoprotein particles in cerebrospinal fluid and lower brain levels of apoE. Overexpression of ABCA1 reduces amyloid deposition, and increases lipidated apoE protein in a transgenic mouse model of APP (Wahrle et al., 2008). Conversely, deletion of ABCA1 dramatically increases Aβ accumulation in several different transgenic mouse models of APP (Hirsch-Reinshagen et al., 2005; Liu et al., 2008; Wahrle et al., 2005). These studies therefore show that elevated ABCA1 enhances Aβ clearance. We observed that HP-β-CD administration significantly increased ABCA1 expression levels and decreased the deposition of both 6E10-immunostained and ThS-positive plaques in the brains of Tg19959 mice. It is therefore reasonable to speculate that HP-β-CD administration to Tg19959 mice reduces Aβ deposition in the brains not only by reducing amyloidogenic processing of APP, but also by enhancing ABCA1 mediated Aβ clearance. We did not observe changes in expression levels of genes that are regulated by SREBP and that encode key proteins involved in cholesterol synthesis.

We hypothesize that HP-β-CD up-regulates ABCA1 and NPC1 by affecting cholesterol metabolism and activating LXRs, which are known to regulate ABCA1 and to affect NPC1 (Rigamonti et al., 2005). Elevated ABCA1 expression enhances cholesterol transport and apoE lipidation, and more importantly, increases Aβ clearance. It was recently shown that activation of LXR/RXR using bexarotene dramatically reduced plaque burden in an apoE-dependent manner (Cramer et al., 2012). This effect on cholesterol transport and Aβ clearance distinguishes the mechanism of HP-β-CD from that of cholesterol synthesis inhibitors such as statins, which have had no benefit in the treatment of AD (Jick et al., 2000; Blauw et al., 2001; McGuinness et al., 2009), and may have important consequences for its development and utility as a therapy for AD. A human protocol for intrathecal CD administration in NPC disease was approved in 2010 (Hastings, 2010).

Because our cell and mouse models of AD are based on overexpression of APP as the causative abnormality, we have focused on the effects of HP-β-CD on Aβ levels. However, we cannot rule out the possibility that HP-β-CD could also have beneficial effects not involving Aβ. For example, there was a nonsignificant trend for wild-type mice treated with HP-β-CD to remember the platform location better in the MWM probe trial than wild-type mice treated with saline control.

In conclusion, we found that 4 mo of subcutaneous administration of HP-β-CD to Tg19959 mice significantly improved memory deficits and reduced amyloid deposition, microgliosis, and tau immunoreactive dystrophic neurites. These effects occurred at least in part by reducing amyloidogenic processing of APP and enhancing ABCA1-mediated Aβ clearance. The present data suggest that HP-β-CD may have therapeutic potential for the treatment of AD.

MATERIALS AND METHODS

Experimental animals and cell lines. Tg19959 mice were obtained from G. Carlson (McLaughlin Research Institute, Great Falls, MT). Tg19959

mice were constructed by injecting FVB×129S6 F1 embryos with a cosmid insert containing human APP695 with two familial AD mutations (KM670/671NL and V717F), under control of the hamster PrP promoter. All experiments were approved by the Institutional Animal Care and Use Committee at Weill-Cornell Medical College.

Mouse N2a neuroblastoma cells stably transfected with human APP695 carrying the 670/671 Swedish mutation (SwN2a) were grown as described previously (Yao et al., 2010).

HP-β-CD treatment in cells. 10 mM HP-β-CD stock solution was made in 1XPBS. SwN2a and N2a cells were treated with HP-β-CD (5 mM) in serum-free medium at different incubation times. To measure Aβ levels, SwN2a cells were recovered in serum-free medium for 5 or 24 h after HP-β-CD treatment.

Filipin staining analysis and colocalization with intracellular markers. Filipin was prepared in DMSO (50 mg/ml) and stored at −20°C. Cells were fixed in 4% PFA for 30 min. For filipin staining, separate permeabilization of cells or brain slices is not needed because filipin itself permeabilizes the cells. The stock solution was diluted in PBS (1:100–1:500), and the cells or brain slices were incubated for 15 min or 2 h at room temperature. Then the cells or brain slices were washed in PBS 3 times for 5 min. Anti-fading reagent (Fluoromount-G; SouthernBiotech) was used in the mounting medium. Filipin was detected using λex = 360 nm and λem = 460 nm. A fluorescence microscope connected to a charge-coupled device camera was used, and images were taken using Metamorph (Molecular Devices). To analyze the images, we used ImageJ (National Institutes of Health) to apply a 70% threshold onto the images (Yao et al., 2006), and quantified the alteration of filipin intensity of SwN2a cells with and without HP-β-CD treatment.

We used protein disulfide isomerase (PDI) as a marker for endoplasmic reticulum (mouse monoclonal anti-PDI; Abcam; ab2792), and manganese superoxide dismutase (MnSOD) as a marker for mitochondria (rabbit polyclonal anti-MnSOD; Millipore; 06–984).

To visualize endocytic recycling compartments, we labeled cells with Alexa Fluor 546-transferrin (Tf) for 10 min in serum-free medium supplemented with 0.5% ovalbumin and 20 mM Hepes at 37°C. Cells were washed three times with 150 mM NaCl, 20 mM HEPES, 1 mM $CaCl_2$, 5 mM KCl, 1 mM $MgCl_2$, 0.2% glucose. Cells were then returned to medium 2 (growth medium containing 5% FBS, 20 µg/ml of Fe^2Tf [unlabeled], 20 µM glucose) for 15 min at 37°C. HP-β-CD was added in medium 2. Finally, cells were washed three times with PBS and fixed in 4% PFA.

Cholesterol extraction from SwN2a cells. Six-well plates of SwN2a cells were treated with and without HP-β-CD for 15 min. Cells were washed 3 times with Hank's buffer, and then 800 µl of hexane/isopropanol (3:2 vol/vol) containing β-sitosterol (internal standard, 5 µg of β-sitosterol per well) was added. Lipids were extracted for 30 min under gentle shaking at room temperature. Lipid extracts were transferred to 12 × 75 mm borosilicate glass culture tubes and dried under Argon. The extraction was repeated, and 50 µl hexane was added per tube, vortexed, and then transferred into glass vials for separation and analysis on GC-Mass Spec. The levels of cholesterol/gram protein were calculated and plotted.

HP-β-CD administration to mice. Mice were treated with HP-β-CD (4,000 mg/kg) by subcutaneous injection twice weekly. HP-β-CD was provided as a 20% (wt/vol) solution in isotonic saline, whereas isotonic saline alone served as the control. The injection of HP-β-CD in the mice was started at P7, and the duration of the treatment was 4 mo. The mice were sacrificed after undergoing Morris water maze testing, a total of 8 d after last injection.

Morris water maze. Spatial learning and memory were analyzed using the Morris water maze. The mice were handled daily, starting 1 wk before behavioral testing, to habituate them. During the acquisition period, visual cues were arranged in the room. The hidden platform was located in the middle of the northwest quadrant. Each day, mice were placed next to and facing the wall of the basin in four starting positions: north, east, south, and west, corresponding to four successive trials per day. The duration of a trial was 60 s, with an inter-trial interval of 60 min. Whenever the mouse failed to reach the platform within 60 s, it was placed on the platform by the experimenter for 10 s. Latencies before reaching the platform were recorded for 5 d and analyzed.

A probe trial was assessed 24 h after the last trial of the acquisition period, removing the platform from the pool. Mice were released on the north side for a single trial of 60 s, during which the time spent in the area of the platform was measured. The velocity was also measured.

Visible platform testing was performed over 2 d with 4 trials per day. In this cued test, a pole was added on the platform, and its location was changed between each trial. The duration of a trial was 60 s, with an inter-trial interval of 60 min. Latencies before reaching the platform were recorded and averaged.

Sample preparation from brains and cells. After being tested in the MWM (8 d after last CD injection), the mice were deeply anesthetized with intraperitoneal sodium pentobarbital and transcardially perfused with ice-cold saline. The brains were removed and dissected on ice. One hemisphere was used for histological analysis and the other hemisphere was used for subsequent protein extraction or TRIzol RNA extraction (Invitrogen). Brain tissues were homogenized in lysis buffer containing 1% SDS + 0.5% NP-40 and protease inhibitors (Roche) for Western blot analysis. Cells were homogenized and prepared in TRIzol for RNA extraction and in RIPA buffer or 1% Triton in PBS for protein extraction. Protein concentrations were determined by BCA protein assay (Thermo Fisher Scientific).

Western blot analysis. Samples with equal amount of protein were separated by Tricine-SDS gel electrophoresis and transferred to PVDF membranes using the iBlot dry blotting system (Invitrogen). Membranes were blocked with 5% milk/0.1% Tween 20 in TBS for 1 h at room temperature, followed by incubation with primary antibodies overnight at 4°C. Signals were detected using HRP-conjugated secondary antibodies and enhanced chemiluminescence (Thermo Fisher Scientific). Blots were scanned at 600 dpi and densitometry was performed using ImageJ. We used the following antibodies: mouse monoclonal anti-tubulin (Sigma-Aldrich; 1:10000), mouse anti-β amyloid1-16 (6E10) monoclonal antibody (Covance; 1:1,000), rabbit anti-APP C-terminal antibody (EMD Millipore), HRP-conjugated goat anti–mouse IgG (1:2,000), and goat anti–rabbit IgG (1:3,000; KPL).

ELISA. Aβ42 and Aβ40 levels were quantified using commercial ELISA kits (Invitrogen; KHB3441 and KMB3481). The manufacturer's protocol was followed to measure Aβ levels in cell extracts, medium from SwN2a cells, and brain extracts from mice. Medium from SwN2a cells was diluted 1:1 in diluents, and brain extracts were diluted 1:100 in diluents, and then loaded onto the plate for analysis. Each sample was run in duplicate, and the experiments were repeated at least twice.

Immunohistology. The mice which had been assessed behaviorally were deeply anesthetized with intraperitoneal sodium pentobarbital and transcardially perfused with ice-cold saline. Brains were post-fixed in 4% paraformaldehyde in PBS for at least 24 h. The brain tissues were cut in 35-µm sections and immunostained using the avidin–biotin complex peroxidase method and visualized after DAB (diaminobenzidine) incubation for 5 min (Vector Laboratories). For each animal, five sections were analyzed. For amyloid deposits, brain sections were labeled with the anti-Aβ42 rabbit polyclonal antibody AB5078P (1:1,000; EMD Millipore). For microglial activation, adjacent sections were also labeled with anti–CD-11b rat monoclonal antibody (1:100; Serotec). For phosphorylated tau, sections were labeled with AT8 antibody (1:500; Thermo Fisher Scientific). For cathepsin D, sections were labeled with RU4 antibody (gift from R. Nixon, New York University School of Medicine/Nathan Kline Institute, New York, NY). Using ImageJ version 1.63 software, the percentage areas occupied by AB5078P immunoreactive amyloid plaques and by CD11b immunoreactive reactive microglia per 0.75 mm^2 were calculated.

ThS staining. Floating sections from Tg19959 were washed and incubated in 1% Triton-PBS for 15 min. Sections were then washed with PBS and stained for 5 min with a solution of 0.05% Thioflavin S (ThS) in 50% ethanol. Finally, sections were washed in 50% ethanol, and then in water. The fluorescence of ThS was detected using λex = 488 nm with fluorescence microscopy. The area of ThS fluorescence was determined using ImageJ and expressed as a fraction of total area.

Quantitation of genes by RT-PCR. RNA was extracted from 4-mo-old mouse brains using the TRIzol protocol (Invitrogen). Total RNA (1 µg) was then reverse transcribed into cDNA using the High Capacity cDNA Reverse Transcription kit (Applied Biosystems), with the addition of nuclease-free deionized water. Reverse transcription was performed according to the manufacturer's protocol. A total of 30 ng of cDNA was loaded into each well of the PCR plate. The cDNA was analyzed in duplicate by real-time quantitative PCR using the ABI Prism 7000 Sequence Detection System (Applied Biosystems, USA) and detected with Power SYBR Green Master Mix (Applied Biosystems, USA. Primer sequences were obtained from previous publications (Liu et al., 2009; Kågedal et al., 2010). For each sample, the cycle number Ct to reach threshold fluorescence was determined in duplicate for each mRNA and actin. To determine relative amounts of mRNA in Tg19959 mice versus WT mice, data are presented using the $2^{-\Delta\Delta Ct}$ method.

Statistics. Unpaired comparisons between two groups were performed using Student's *t* test assuming equal or unequal variances as determined by F-test. Comparisons involving more than two groups were performed using one way analysis of variance (ANOVA) with post hoc Tukey testing to adjust for multiple comparisons. For the acquisition period and visible platform of the Morris water maze, we used two-way ANOVA to compare four experimental groups for 5 d of hidden platform training and 2 d of visual platform training. For the probe trial of the Morris water maze, we used a one-way ANOVA for each of four experimental groups to compare their total time spending in the area of platform. *, $P < 0.01$; **, $P < 0.05$; ***, $P < 0.001$; ****, $P < 0.0001$. Calculations were performed using Excel 2003 (Microsoft) and Prism (GraphPad).

We thank Dr. Xiaoyan Hu for insightful comments and experimental support, Dr. Ralph Nixon for his generous gift of RU4 antibody, and Dr. J David Warren and Milstein Chemistry Core Facility (Weill Cornell Medical College) for help with GC Mass Spectrometry.

This work was supported by National Institutes of Health (R01 AG20729 to M.T. Lin and P01 AG14930 to G. Gibson).

The authors have no conflicting financial interests.

Author contributions: J. Yao and M.F. Beal planned the project. J. Yao designed, performed, and analyzed the results of most of the experiments. D. Ho assisted in animal-related experiments. N.Y. Calingasan performed the histological staining and analysis. N.H. Pipalia performed GC-mass spectometry and helped with fluorescent staining and analysis. M.T. Lin helped with data interpretation and figure preparation. J. Yao, M.T. Lin, and M.F. Beal wrote the manuscript.

Submitted: 11 June 2012
Accepted: 17 October 2012

REFERENCES

Aqul, A., B. Liu, C.M. Ramirez, A.A. Pieper, S.J. Estill, D.K. Burns, B. Liu, J.J. Repa, S.D. Turley, and J.M. Dietschy. 2011. Unesterified cholesterol accumulation in late endosomes/lysosomes causes neurodegeneration and is prevented by driving cholesterol export from this compartment. *J. Neurosci.* 31:9404–9413. http://dx.doi.org/10.1523/JNEUROSCI.1317-11.2011

Bahr, B.A., B. Abai, C.M. Gall, P.W. Vanderklish, K.B. Hoffman, and G. Lynch. 1994. Induction of beta-amyloid-containing polypeptides in hippocampus: evidence for a concomitant loss of synaptic proteins and interactions with an excitotoxin. *Exp. Neurol.* 129:81–94. http://dx.doi.org/10.1006/exnr.1994.1149

Barrett, P.J., Y. Song, W.D. Van Horn, E.J. Hustedt, J.M. Schafer, A. Hadziselimovic, A.J. Beel, and C.R. Sanders. 2012. The amyloid precursor protein has a flexible transmembrane domain and binds cholesterol. *Science.* 336:1168–1171. http://dx.doi.org/10.1126/science.1219988

Bełtowski, J. 2008. Liver X receptors (LXR) as therapeutic targets in dyslipidemia. *Cardiovasc Ther.* 26:297–316. http://dx.doi.org/10.1111/j.1755-5922.2008.00062.x

Blauw, G.J., J. Shepherd, and M.B. Murphy; PROSPER study group. 2001. Dementia and statins. PROSPER study group. *Lancet.* 357:881. http://dx.doi.org/10.1016/S0140-6736(05)71808-0

Brown, M.S., and J.L. Goldstein. 1997. The SREBP pathway: regulation of cholesterol metabolism by proteolysis of a membrane-bound transcription factor. *Cell.* 89:331–340. http://dx.doi.org/10.1016/S0092-8674(00)80213-5

Cordy, J.M., N.M. Hooper, and A.J. Turner. 2006. The involvement of lipid rafts in Alzheimer's disease. *Mol. Membr. Biol.* 23:111–122. http://dx.doi.org/10.1080/09687860500496417

Coskun, U., and K. Simons. 2010. Membrane rafting: from apical sorting to phase segregation. *FEBS Lett.* 584:1685–1693. http://dx.doi.org/10.1016/j.febslet.2009.12.043

Cramer, P.E., J.R. Cirrito, D.W. Wesson, C.Y. Lee, J.C. Karlo, A.E. Zinn, B.T. Casali, J.L. Restivo, W.D. Goebel, M.J. James, et al. 2012. ApoE-directed therapeutics rapidly clear β-amyloid and reverse deficits in AD mouse models. *Science.* 335:1503–1506. http://dx.doi.org/10.1126/science.1217697

Davidson, C.D., N.F. Ali, M.C. Micsenyi, G. Stephney, S. Renault, K. Dobrenis, D.S. Ory, M.T. Vanier, and S.U. Walkley. 2009. Chronic cyclodextrin treatment of murine Niemann-Pick C disease ameliorates neuronal cholesterol and glycosphingolipid storage and disease progression. *PLoS ONE.* 4:e6951. http://dx.doi.org/10.1371/journal.pone.0006951

Di Paolo, G., and T.W. Kim. 2011. Linking lipids to Alzheimer's disease: cholesterol and beyond. *Nat. Rev. Neurosci.* 12:284–296. http://dx.doi.org/10.1038/nrn3012

Dickson, T.C., C.E. King, G.H. McCormack, and J.C. Vickers. 1999. Neurochemical diversity of dystrophic neurites in the early and late stages of Alzheimer's disease. *Exp. Neurol.* 156:100–110. http://dx.doi.org/10.1006/exnr.1998.7010

Ehehalt, R., P. Keller, C. Haass, C. Thiele, and K. Simons. 2003. Amyloidogenic processing of the Alzheimer β-amyloid precursor protein depends on lipid rafts. *J. Cell Biol.* 160:113–123. http://dx.doi.org/10.1083/jcb.200207113

Fontaine, C., E. Rigamonti, B. Pourcet, H. Duez, C. Duhem, J.C. Fruchart, G. Chinetti-Gbaguidi, and B. Staels. 2008. The nuclear receptor Rev-erbalpha is a liver X receptor (LXR) target gene driving a negative feedback loop on select LXR-induced pathways in human macrophages. *Mol. Endocrinol.* 22:1797–1811. http://dx.doi.org/10.1210/me.2007-0439

Guirland, C., S. Suzuki, M. Kojima, B. Lu, and J.Q. Zheng. 2004. Lipid rafts mediate chemotropic guidance of nerve growth cones. *Neuron.* 42:51–62. http://dx.doi.org/10.1016/S0896-6273(04)00157-6

Hartmann, T., J. Kuchenbecker, and M.O. Grimm. 2007. Alzheimer's disease: the lipid connection. *J. Neurochem.* 103(Suppl 1):159–170. http://dx.doi.org/10.1111/j.1471-4159.2007.04715.x

Hastings, C. 2010. Request for intrathecal delivery of Hpbcd for Niemann Pick type C patients. http://addiandcassi.com/wordpress/wp-content/uploads/Hempel-Cyclodextrin-Intrathecal-FDA-Filing-2010-Aug.pdf Accessed. September 2010.

Hirsch-Reinshagen, V., L.F. Maia, B.L. Burgess, J.F. Blain, K.E. Naus, S.A. McIsaac, P.F. Parkinson, J.Y. Chan, G.H. Tansley, M.R. Hayden, et al. 2005. The absence of ABCA1 decreases soluble ApoE levels but does not diminish amyloid deposition in two murine models of Alzheimer disease. *J. Biol. Chem.* 280:43243–43256. http://dx.doi.org/10.1074/jbc.M508781200

Jessup, W., I.C. Gelissen, K. Gaus, and L. Kritharides. 2006. Roles of ATP binding cassette transporters A1 and G1, scavenger receptor BI and membrane lipid domains in cholesterol export from macrophages. *Curr. Opin.*

Lipidol. 17:247–257. http://dx.doi.org/10.1097/01.mol.0000226116.35555.eb

Jick, H., G.L. Zornberg, S.S. Jick, S. Seshadri, and D.A. Drachman. 2000. Statins and the risk of dementia. *Lancet.* 356:1627–1631. http://dx.doi.org/10.1016/S0140-6736(00)03155-X

Kågedal, K., W.S. Kim, H. Appelqvist, S. Chan, D. Cheng, L. Agholme, K. Barnham, H. McCann, G. Halliday, and B. Garner. 2010. Increased expression of the lysosomal cholesterol transporter NPC1 in Alzheimer's disease. *Biochim. Biophys. Acta.* 1801:831–838. http://dx.doi.org/10.1016/j.bbalip.2010.05.005

Kim, W.S., A.S. Rahmanto, A. Kamili, K.A. Rye, G.J. Guillemin, I.C. Gelissen, W. Jessup, A.F. Hill, and B. Garner. 2007. Role of ABCG1 and ABCA1 in regulation of neuronal cholesterol efflux to apolipoprotein E discs and suppression of amyloid-beta peptide generation. *J. Biol. Chem.* 282:2851–2861. http://dx.doi.org/10.1074/jbc.M607831200

Kivipelto, M., E.L. Helkala, M.P. Laakso, T. Hänninen, M. Hallikainen, K. Alhainen, H. Soininen, J. Tuomilehto, and A. Nissinen. 2001. Midlife vascular risk factors and Alzheimer's disease in later life: longitudinal, population based study. *BMJ.* 322:1447–1451. http://dx.doi.org/10.1136/bmj.322.7300.1447

Kodam, A., M. Maulik, K. Peake, A. Amritraj, K.S. Vetrivel, G. Thinakaran, J.E. Vance, and S. Kar. 2010. Altered levels and distribution of amyloid precursor protein and its processing enzymes in Niemann-Pick type C1-deficient mouse brains. *Glia.* 58:1267–1281. http://dx.doi.org/10.1002/glia.21001

Koldamova, R., M. Staufenbiel, and I. Lefterov. 2005a. Lack of ABCA1 considerably decreases brain ApoE level and increases amyloid deposition in APP23 mice. *J. Biol. Chem.* 280:43224–43235. http://dx.doi.org/10.1074/jbc.M504513200

Koldamova, R.P., I.M. Lefterov, M. Staufenbiel, D. Wolfe, S. Huang, J.C. Glorioso, M. Walter, M.G. Roth, and J.S. Lazo. 2005b. The liver X receptor ligand T0901317 decreases amyloid beta production in vitro and in a mouse model of Alzheimer's disease. *J. Biol. Chem.* 280:4079–4088. http://dx.doi.org/10.1074/jbc.M411420200

Lee, S.J., U. Liyanage, P.E. Bickel, W. Xia, P.T. Lansbury Jr., and K.S. Kosik. 1998. A detergent-insoluble membrane compartment contains A beta in vivo. *Nat. Med.* 4:730–734. http://dx.doi.org/10.1038/nm0698-730

Liu, B., H. Li, J.J. Repa, S.D. Turley, and J.M. Dietschy. 2008. Genetic variations and treatments that affect the lifespan of the NPC1 mouse. *J. Lipid Res.* 49:663–669. http://dx.doi.org/10.1194/jlr.M700525-JLR200

Liu, B., S.D. Turley, D.K. Burns, A.M. Miller, J.J. Repa, and J.M. Dietschy. 2009. Reversal of defective lysosomal transport in NPC disease ameliorates liver dysfunction and neurodegeneration in the $npc1^{-/-}$ mouse. *Proc. Natl. Acad. Sci. USA.* 106:2377–2382. http://dx.doi.org/10.1073/pnas.0810895106

Liu, B., C.M. Ramirez, A.M. Miller, J.J. Repa, S.D. Turley, and J.M. Dietschy. 2010. Cyclodextrin overcomes the transport defect in nearly every organ of NPC1 mice leading to excretion of sequestered cholesterol as bile acid. *J. Lipid Res.* 51:933–944. http://dx.doi.org/10.1194/jlr.M000257

Maulik, M., B. Ghoshal, J. Kim, Y. Wang, J. Yang, D. Westaway, and S. Kar. 2012. Mutant human APP exacerbates pathology in a mouse model of NPC and its reversal by a β-cyclodextrin. *Hum. Mol. Genet.* 21:4857–4875. http://dx.doi.org/10.1093/hmg/dds322

Maxwell, K.N., R.E. Soccio, E.M. Duncan, E. Sehayek, and J.L. Breslow. 2003. Novel putative SREBP and LXR target genes identified by microarray analysis in liver of cholesterol-fed mice. *J. Lipid Res.* 44:2109–2119. http://dx.doi.org/10.1194/jlr.M300203-JLR200

McGuinness, B., D. Craig, R. Bullock, and P. Passmore. 2009. Statins for the prevention of dementia. *Cochrane Database Syst. Rev.* (2): CD003160.

Mesmin, B., and F.R. Maxfield. 2009. Intracellular sterol dynamics. *Biochim. Biophys. Acta.* 1791:636–645. http://dx.doi.org/10.1016/j.bbalip.2009.03.002

Meyer-Luehmann, M., T.L. Spires-Jones, C. Prada, M. Garcia-Alloza, A. de Calignon, A. Rozkalne, J. Koenigsknecht-Talboo, D.M. Holtzman, B.J. Bacskai, and B.T. Hyman. 2008. Rapid appearance and local toxicity of amyloid-beta plaques in a mouse model of Alzheimer's disease. *Nature.* 451:720–724. http://dx.doi.org/10.1038/nature06616

Mondal, M., B. Mesmin, S. Mukherjee, and F.R. Maxfield. 2009. Sterols are mainly in the cytoplasmic leaflet of the plasma membrane and the endocytic recycling compartment in CHO cells. *Mol. Biol. Cell.* 20:581–588. http://dx.doi.org/10.1091/mbc.E08-07-0785

Morgan, D. 2011. Immunotherapy for Alzheimer's disease. *J. Intern. Med.* 269:54–63. http://dx.doi.org/10.1111/j.1365-2796.2010.02315.x

Nixon, R.A. 2004. Niemann-Pick Type C disease and Alzheimer's disease: the APP-endosome connection fattens up. *Am. J. Pathol.* 164:757–761. http://dx.doi.org/10.1016/S0002-9440(10)63163-X

Nixon, R.A., A.M. Cataldo, and P.M. Mathews. 2000. The endosomal-lysosomal system of neurons in Alzheimer's disease pathogenesis: a review. *Neurochem. Res.* 25:1161–1172. http://dx.doi.org/10.1023/A:1007675508413

Peake, K.B., and J.E. Vance. 2012. Normalization of cholesterol homeostasis by 2-hydroxypropyl-β-cyclodextrin in neurons and glia from Niemann-Pick C1 (NPC1)-deficient mice. *J. Biol. Chem.* 287:9290–9298. http://dx.doi.org/10.1074/jbc.M111.326405

Puglielli, L., R.E. Tanzi, and D.M. Kovacs. 2003. Alzheimer's disease: the cholesterol connection. *Nat. Neurosci.* 6:345–351. http://dx.doi.org/10.1038/nn0403-345

Ramirez, C.M., B. Liu, A.M. Taylor, J.J. Repa, D.K. Burns, A.G. Weinberg, S.D. Turley, and J.M. Dietschy. 2010. Weekly cyclodextrin administration normalizes cholesterol metabolism in nearly every organ of the Niemann-Pick type C1 mouse and markedly prolongs life. *Pediatr. Res.* 68:309–315. http://dx.doi.org/10.1203/PDR.0b013e3181ee4dd2

Ramirez, C.M., B. Liu, A. Aqul, A.M. Taylor, J.J. Repa, S.D. Turley, and J.M. Dietschy. 2011. Quantitative role of LAL, NPC2, and NPC1 in lysosomal cholesterol processing defined by genetic and pharmacological manipulations. *J. Lipid Res.* 52:688–698. http://dx.doi.org/10.1194/jlr.M013789

Rigamonti, E., L. Helin, S. Lestavel, A.L. Mutka, M. Lepore, C. Fontaine, M.A. Bouhlel, S. Bultel, J.C. Fruchart, E. Ikonen, et al. 2005. Liver X receptor activation controls intracellular cholesterol trafficking and esterification in human macrophages. *Circ. Res.* 97:682–689. http://dx.doi.org/10.1161/01.RES.0000184678.43488.9f

Sato, R. 2010. Sterol metabolism and SREBP activation. *Arch. Biochem. Biophys.* 501:177–181. http://dx.doi.org/10.1016/j.abb.2010.06.004

Schmitz, G., and W. Drobnik. 2002. ATP-binding cassette transporters in macrophages: promising drug targets for treatment of cardiovascular disease. *Curr. Opin. Investig. Drugs.* 3:853–858.

Simons, M., P. Keller, B. De Strooper, K. Beyreuther, C.G. Dotti, and K. Simons. 1998. Cholesterol depletion inhibits the generation of beta-amyloid in hippocampal neurons. *Proc. Natl. Acad. Sci. USA.* 95:6460–6464. http://dx.doi.org/10.1073/pnas.95.11.6460

Sparks, D.L., R.J. Kryscio, D.J. Connor, M.N. Sabbagh, L.M. Sparks, Y. Lin, and C. Liebsack. 2010. Cholesterol and cognitive performance in normal controls and the influence of elective statin use after conversion to mild cognitive impairment: results in a clinical trial cohort. *Neurodegener. Dis.* 7:183–186. http://dx.doi.org/10.1159/000295660

Terwel, D., K.R. Steffensen, P.B. Verghese, M.P. Kummer, J.A. Gustafsson, D.M. Holtzman, and M.T. Heneka. 2011. Critical role of astroglial apolipoprotein E and liver X receptor-α expression for microglial Aβ phagocytosis. *J. Neurosci.* 31:7049–7059. http://dx.doi.org/10.1523/JNEUROSCI.6546-10.2011

Vetrivel, K.S., and G. Thinakaran. 2010. Membrane rafts in Alzheimer's disease beta-amyloid production. *Biochim. Biophys. Acta.* 1801:860–867. http://dx.doi.org/10.1016/j.bbalip.2010.03.007

Wahrle, S., P. Das, A.C. Nyborg, C. McLendon, M. Shoji, T. Kawarabayashi, L.H. Younkin, S.G. Younkin, and T.E. Golde. 2002. Cholesterol-dependent gamma-secretase activity in buoyant cholesterol-rich membrane microdomains. *Neurobiol. Dis.* 9:11–23. http://dx.doi.org/10.1006/nbdi.2001.0470

Wahrle, S.E., H. Jiang, M. Parsadanian, R.E. Hartman, K.R. Bales, S.M. Paul, and D.M. Holtzman. 2005. Deletion of Abca1 increases Abeta deposition in the PDAPP transgenic mouse model of Alzheimer

disease. *J. Biol. Chem.* 280:43236–43242. http://dx.doi.org/10.1074/jbc.M508780200

Wahrle, S.E., H. Jiang, M. Parsadanian, J. Kim, A. Li, A. Knoten, S. Jain, V. Hirsch-Reinshagen, C.L. Wellington, K.R. Bales, et al. 2008. Overexpression of ABCA1 reduces amyloid deposition in the PDAPP mouse model of Alzheimer disease. *J. Clin. Invest.* 118:671–682.

Wyss-Coray, T. 2006. Inflammation in Alzheimer disease: driving force, bystander or beneficial response? *Nat. Med.* 12:1005–1015.

Xiong, H., D. Callaghan, A. Jones, D.G. Walker, L.F. Lue, T.G. Beach, L.I. Sue, J. Woulfe, H. Xu, D.B. Stanimirovic, and W. Zhang. 2008. Cholesterol retention in Alzheimer's brain is responsible for high beta- and gamma-secretase activities and Abeta production. *Neurobiol. Dis.* 29:422–437. http://dx.doi.org/10.1016/j.nbd.2007.10.005

Yang, D.S., P. Stavrides, P.S. Mohan, S. Kaushik, A. Kumar, M. Ohno, S.D. Schmidt, D. Wesson, U. Bandyopadhyay, Y. Jiang, et al. 2011. Reversal of autophagy dysfunction in the TgCRND8 mouse model of Alzheimer's disease ameliorates amyloid pathologies and memory deficits. *Brain.* 134:258–277. http://dx.doi.org/10.1093/brain/awq341

Yao, J., Y. Sasaki, Z. Wen, G.J. Bassell, and J.Q. Zheng. 2006. An essential role for beta-actin mRNA localization and translation in Ca2+-dependent growth cone guidance. *Nat. Neurosci.* 9:1265–1273. http://dx.doi.org/10.1038/nn1773

Yao, J., T. Hennessey, A. Flynt, E. Lai, M.F. Beal, and M.T. Lin. 2010. MicroRNA-related cofilin abnormality in Alzheimer's disease. *PLoS ONE.* 5:e15546. http://dx.doi.org/10.1371/journal.pone.0015546

Zhang, L., R. Sheng, and Z. Qin. 2009. The lysosome and neurodegenerative diseases. *Acta Biochim. Biophys. Sin. (Shanghai).* 41:437–445. http://dx.doi.org/10.1093/abbs/gmp031

Zidovetzki, R., and I. Levitan. 2007. Use of cyclodextrins to manipulate plasma membrane cholesterol content: evidence, misconceptions and control strategies. *Biochim. Biophys. Acta.* 1768:1311–1324. http://dx.doi.org/10.1016/j.bbamem.2007.03.026